ISSN 1066-3622, Radiochemistry, 2018, Vol. 60, No. 1, pp. 70–78. © Pleiades Publishing, Inc., 2018.
Original Russian Text © S.E. Vinokurov, S.A. Kulikova, V.V. Krupskaya, B.F. Myasoedov, 2018, published in Radiokhimiya, 2018, Vol. 60, No. 1, pp. 66–73.

Magnesium Potassium Phosphate Compound for Radioactive Waste Immobilization: Phase Composition, Structure, and Physicochemical and Hydrolytic Durability

S. E. Vinokurov*[a], S. A. Kulikova[a], V. V. Krupskaya[b,c], and B. F. Myasoedov[a]

[a] *Vernadsky Institute of Geochemistry and Analytical Chemistry, Russian Academy of Sciences, ul. Kosygina 19, Moscow, 119991 Russia*

[b] *Institute of Geology of Ore Deposits, Petrography, Mineralogy, and Geochemistry, Russian Academy of Sciences, Staromonetnyi per. 35, Moscow, 119017 Russia*

[c] *Geological Faculty, Moscow State University, Moscow, Russia*

**e-mail: vinokurov.geokhi@gmail.com*

Received May 22, 2017

Abstract—Low-temperature mineral-like magnesium potassium phosphate (MPP) compounds were synthesized in the course of immobilization of nitric acid solutions containing cesium, strontium, sodium, ammonium, lanthanum, and iron as simulated radioactive waste (RW). The phase composition and structure of the compounds and the distribution of the RW components were studied. The mechanical strength (15 ± 3 MPa), heat resistance (up to 450°C), and radiation resistance (absorbed dose 1 MGy) of the compounds were evaluated in accordance with the existing regulations. The MPP compound exhibits high hydrolytic durability: The differential leach rate of ^{239}Pu and ^{152}Eu on the 28th day, measured in accordance with GOST (State Standard) R 52 126–2003, is 2.1×10^{-6} and 1.4×10^{-4} g cm^{-2} day^{-1}, respectively. Introduction of wollastonite into the compound decreases the radionuclide leach rate by a factor of up to 5. The MPP compound shows promise for industrial solidification of liquid RW, including high-level highly saline multicomponent actinide-containing waste.

Keywords: mineral-like phosphate compounds, radioactive waste solidification, leaching

DOI: 10.1134/S1066362218010125

Prospects for the development of nuclear industry depend on the efficiency of the management of radioactive waste (RW) formed in the nuclear fuel cycle and accumulated in the course of implementation of defense programs in the past. The RW management concept that is being implemented today in Russia involves stopping the RW discharge into open aquatic systems. The waste should be converted to a stable solidified form suitable for long-term controlled storage and/or disposal. Various high- and low-temperature host materials have been developed for RW immobilization, depending on the kind and radiotoxicity of RW [1, 2]. The quality requirements to the host materials are formulated in NP-019-15 document [3]. Cement [4] and glassy [5] compounds are considered as host materials for immobilization of intermediate- (ILW) and high-level (HLW) actinide-containing RW.

Cementation has found wide use in nuclear industry for management of various kinds of RW. Mixing of Portland cement with water gives cement mortar, which sets and transforms into cement stone as the clinker minerals undergo hydration. The drawbacks of this method are relatively low degree of incorporation of RW salts into the cement and low levels of hydrolytic durability and frost resistance of cement stone with the incorporated waste salts.

Vitrification is today the only HLW management technology brought to industrial implementation [6]. Borosilicate glass is used for this purpose in the majority of countries, and a glass on the sodium aluminophosphate base is used today in Russia for HLW solidification after reprocessing spent nuclear fuel from WWER-440 (440-MW_{el} water-cooled water-moderated energy reactor) reactors at the RT-1 plant of

the Mayak Production Association [7]. The main drawbacks of this method are low levels of chemical durability and crystallization resistance of the glass at elevated temperatures and short operation life and high cost of the melting equipment and gas treatment systems.

The urgency of searching for new effective host materials is determined by the need for immobilizing considerably expanded range of RW of complex chemical and radionuclidic compositions, containing highly toxic long-lived actinides and fission products. It should be noted that management of some kinds of RW (e.g., those with high content of sulfates or ammonium) using standard cementation and vitrification methods does not comply with the requirements of [3].

Ceramic (mineral-like) host materials, including multiphase materials [8] and materials based on individual crystalline phases [9, 10], are considered as an alternative to glasses for immobilization of RW containing long-lived radionuclides. High-temperature methods for preparing such host materials (cold and hot pressing–sintering, cold crucible induction melting [11], self-propagating high-temperature synthesis [12], UHF heating [13], etc.) should involve a radiation-hazardous preliminary step of waste calcination. These procedures also impose very stringent requirements upon the quality of the mineral-forming charge. Therefore, low-temperature mineral-like phosphate host materials prepared at room temperature in aqueous solution, as a rule, by the reaction of metal(II) oxides (MgO, ZnO, FeO, CaO) with H_3PO_4 or its derivatives [e.g., metal(I) or ammonium (di)hydrogen phosphates] are of particular interest. Such host materials have crystalline structure similar to ceramics [14–17]. Some low-temperature phosphate materials are widely used, e.g., in dentistry. They are also considered as structural materials, efficient radiation-protective shields, or bioceramics [18].

One of the most promising low-temperature materials for RW immobilization is magnesium potassium phosphate (MPP) $MgKPO_4 \cdot 6H_2O$, a synthetic analog of K-struvite natural mineral [19] prepared at room temperature by acid–base reaction:

$$MgO + KH_2PO_4 + 5H_2O = MgKPO_4 \cdot 6H_2O. \quad (1)$$

The MPP host material has noticeable advantages over Portland cement, consisting primarily in higher solution/binder ratio (usually up to 0.8 L kg^{-1}) with high degree of filling with RW salts (up to 30 wt %) and in the possibility of curing liquid waste with pH varying in a wide range [20–23]. It should be noted that possible use of such host materials for ILW and HLW management, in contrast to the use of glass or ceramics, does not require construction of expensive high-temperature electric furnaces or special melters whose decommissioning is a particular radioecological problem, yet unsolved.

Previously we demonstrated the efficiency of using MPP host material for immobilization of "historical" RW [24–28]. Proceeding with studies in this field, we examined the phase composition, structure, mechanical strength, radiation resistance, and thermal and hydrolytic durability of various compounds based on MPP host material (hereinafter, MPP compounds), including those formed in the course of solidification of a highly saline solution simulating industrial actinide-containing ILW.

EXPERIMENTAL

The chemicals used in the experiments were of no less than chemically pure grade.

For preparing samples of MPP compounds by reaction (1), we used MgO (OOO RusKhim) preliminarily calcined at 1300°C for 3 h (specific surface area 6.6 $m^2\ g^{-1}$) and KH_2PO_4 (TD Khimmed) ground to a particle size of 0.15–0.25 mm. The samples were prepared at the $MgO : H_2O : KH_2PO_4$ weight ratio of 1 : 2 : 3. The excess of MgO relative to the stoichiometry of reaction (1) was 10 wt % [28]. To decrease the rate of reaction (1), boric acid was added to the initial mixture in an amount corresponding to its 1.3 ± 0.1 wt % content in the compound.

The influence of the composition of the solution being solidified on the composition and properties of MPP compounds was determined in experiments on immobilization of concentrated aqueous solutions of cesium, strontium, sodium, ammonium, lanthanum, and iron nitrates simulating RW components (Table 1). In addition, we prepared compounds by solidification of a solution simulating the evaporated and neutralized raffinate from final purification of Pu and Np by extraction (MPP-ILW samples in Table 1). This raffinate belongs to the ILW category. The total salinity of the simulated ILW was 589 g L^{-1}, pH 5.6. The MPP-ILW samples were prepared at the solution/binder ratio of 0.65 L kg^{-1}. The activity concentration of ^{152}Eu and

Table 1. Composition of solidified aqueous solutions and content of metals and ammonium in the synthesized samples of MPP compounds

Sample	Salt composition of solidified aqueous solutions, g L^{-1}	Content of metals and ammonium in samples of MPP compounds, wt %
MPP-Cs	$CsNO_3$ 230	Cs 4.8
MPP-Sr	$Sr(NO_3)_2$ 705	Sr 6.7
MPP-NH_4	NH_4NO_3 530	NH_4 3.4
MPP-Na	$NaNO_3$ 458	Na 3.5
MPP-La	$La(NO_3)_3$ 567	La 6.7
MPP-Fe	$Fe(NO_3)_3$ 186	Fe 1.4
MPP-ILW	$NaNO_3$ 108, Na_2SO_4 217, NH_4NO_3 250, $Eu(NO_3)_3$ 14	Na 3.3, NH_4 1.8, Eu 0.2

^{239}Pu in the MPP-ILW samples was 4.0×10^3 and 1.6×10^5 Bq g^{-1}, respectively.

In studying the effect of mineral modifiers on the properties of MPP compounds, we used wollastonite (FW-200, Nordkalk), bentonite (10th Khutor deposit, Khakassia, Russia), and zeolite (Sokirnit, Transcarpathian deposit, clinoptilolite content 70%). The modifiers were preliminarily ground and sieved, and the fraction with the 0.07–0.16 mm particle size was taken.

After gaining the strength in no less than 15 days, we obtained samples of MPP compounds of up to 50 g weight with a density of up to 2.0 g cm^{-3}. The phase composition of the samples was determined by X-ray diffraction (XRD) (Ultima-IV, Rigaku, Japan). The data were interpreted using the Jade 6.5 program package (MDI) with PDF-2 powder database. The sample structure was studied by scanning electron microscopy (SEM) (LEOSupra 50 VP, Carl Zeiss, Germany) and electron probe microanalysis (EPMA) (X-MAX 80, Oxford Instruments, the United Kingdom).

The mechanical strength and resistance to thermal cycling (30 cycles of keeping in the range from –40 to +40°C) of MPP compounds was determined according to [29, 30]. The radiation resistance of the compounds was evaluated after their irradiation at the UELV-10-10-C-70 linear accelerator (Frumkin Institute of Physical Chemistry and Electrochemistry, Russian Academy of Sciences) with a vertically scanning electron beam; the absorbed dose was no less than 1 MGy. Thermal gravimetric analysis and differential scanning calorimetry (TG/DSC) of the samples were performed in air at temperatures of up to 800°C (STA 409 PC Luxx, Netzsch, Germany).

The hydrolytic durability of MPP compounds was determined using the semidynamic test in accordance with GOST (State Standard) R 52126–2003 [31]. The content of ^{239}Pu and ^{152}Eu in solutions after leaching was determined by α- and γ-ray spectrometry, respectively (Canberra spectrometers, the United States), and the contrent of structure-forming elements was determined by inductively coupled plasma atomic emission spectrometry (ICP-AES) (iCAP-6500 Duo, Thermo Scientific, the United Kingdom).

The mechanism of leaching of structure-forming elements (Mg, K, P) from the MPP compound was evaluated in accordance with the de Groot–van der Sloot model [32], which can be presented in the form of the linear relationship

$$\log Y_i = A \log t + \text{const}, \quad (2)$$

where Y_i is the total yield of ith element from the sample during the time of contact with water, mg m^{-2}; t is the contact time, days.

As shown in [33–36], the following mechanisms of element leaching correspond to various values of A in Eq. (2): >0.65, dissolution; 0.35–0.65, diffusion; and <0.35, washout from the sample surface (including the case of subsequent depletion of the surface layer). The quantities Y_i were calculated using Eq. (3):

$$Y_{in} = C_{in}(L/S)t_n^{1/2}/(t_n^{1/2} - t_{n-1}^{1/2}), \quad (3)$$

where C_{in} is the concentration of ith element in the leaching solution by the end of nth period, mg L^{-1}; L/S, ratio of the solution volume to the sample surface area, L m^{-2}; t_n and t_{n-1}, total contact time by the end of nth period and before its beginning, respectively, days.

RESULTS AND DISCUSSION

Phase Composition and Structure of MPP Compounds

The major crystalline phase in the studied samples of both MPP host material itself and MPP compounds

Table 2. Elemental composition (at. %) of MPP host material

Mg	K	P	O	Calculated formula of MPP host material particles
8.0	7.5	7.7	76.8	$MgKPO_4·6H_2O$ (K-struvite)
10.3	6.0	8.8	74.9	$Mg_{1.16}K_{0.68}PO_4·4.5H_2O$
5.9	9.6	9.6	74.9	$Mg_{0.62}KH_{0.76}PO_4·3.8H_2O$[a]

[a] Hydrogen was introduced into the phosphate formula for charge balance.

Table 3. Elemental composition (at. %) of MPP-M compounds containing metals M: MPP-Cs, M = Cs; MPP-Sr, M = Sr; MPP-La, M = La

Sample	Mg	K	P	O	M	Calculated formula of particles of MPP compounds
MPP-Cs	7.9	8.2	8.2	75.2	0.5	$Mg_{0.97}KCs_{0.06}PO_4·5.2H_2O$
	7.7	11.7	10.1	69.1	1.4	$Mg_{0.76}K_{1.16}Cs_{0.14}H_{0.18}PO_4·2.8H_2O$
	7.2	2.2	7.5	77.5	5.6	$Mg_{0.97}K_{0.29}Cs_{0.75}PO_4·6.3H_2O$
	5.8	4.0	10.5	71.7	8.1	$Mg_{0.55}K_{0.38}Cs_{0.77}H_{0.75}PO_4·2.8H_2O$
	7.1	4.8	8.9	55.4	23.8	$Mg_{0.80}K_{0.54}Cs_{2.67}PO_{4.9}·1.3H_2O$
MPP-Sr	7.1	4.4	9.5	75.1	4.0	$Mg_{0.75}K_{0.46}Sr_{0.42}PO_{3.90}·4.0H_2O$ [5.1 $Mg_{1.05}K_{0.64}Sr_{0.42}PO_{3.9}·6.0H_2O + Sr_3(PO_4)_2$]
	7.8	1.7	7.6	78.2	4.7	$Mg_{1.03}K_{0.22}Sr_{0.62}PO_{4.20}·6.0H_2O$
	4.8	1.8	8.0	79.9	5.5	$Mg_{0.6}K_{0.23}Sr_{0.69}PO_{3.91}·6.1H_2O$
MPP-La	11.6	8.7	14.5	64.3	0.7	$Mg_{0.80}K_{0.60}La_{0.05}H_{0.65}PO_4·0.4H_2O$
	4.6	5.2	7.7	79.5	2.8	$Mg_{0.60}K_{0.68}La_{0.36}PO_4·6.3H_2O$
	8.3	10.6	15.1	59.2	6.6	$Mg_{0.55}K_{0.70}La_{0.44}PO_{4.06}$

containing macroamounts of metal and ammonium is the mineral-like analog of K-struvite $MgKPO_4·6H_2O$ or struvite $MgNH_4PO_4·6H_2O$ (samples MPP-NH_4 and MPP-ILW) (Fig. 1). The MgO phase (periclase) is also present owing to the use of excess MgO relative to the stoichiometry of reaction (1). In solidification of aqueous solutions of element nitrates and of simulated ILW solution, the KNO_3 phase (niter) is formed in the compounds (Fig. 1), which suggests replacement of potassium with metal and ammonium cations. This assumption is confirmed by the presence of the corresponding crystalline phosphate phases in the samples, such as $MgCsPO_4·6H_2O$ in the MPP-Cs sample, $Sr_3(PO_4)_2$ in the MPP-Sr sample, $MgNaPO_4·6H_2O$ and Na_3PO_4 (olympite) in the MPP-Na sample, and $LaPO_4·0.5H_2O$ (rhabdophane-La) in the MPP-La sample.

A study of the structure of the MPP host material has shown that it is constituted by crystalline particles with the prevalent size of 2–10 μm (Fig. 2). The mean elemental composition of the host material corresponds to $MgKPO_4·6H_2O$ (Table 2), but the compositions of separate particles can differ. Some areas of the host material are enriched in Mg and P and have the mean composition $Mg_{1.16}K_{0.68}PO_4·4.5H_2O$ (Table 2), which can correspond to a mixture of K-struvite and $Mg_3(PO_4)_2·2.6H_2O$ in 4.3 : 1 molar ratio. On the other hand, we also found Mg-depleted particles with the probable composition $Mg_{0.62}KH_{0.76}PO_4·3.8H_2O$ (Table 2), which corresponds to a mixture of K-struvite and KH_2PO_4 in 1.6 : 1 molar ratio. However, an intrinsic phase of unchanged KH_2PO_4 has not been revealed by X-ray diffraction (Fig. 1). Nevertheless, the presence of this phase in a small amount (usually no more than 1–2 wt %) cannot be ruled out.

Distribution of Elements in MPP Compounds

Analysis of the elemental cards of MPP compounds confirms that potassium is concentrated in the samples in a separate potassium nitrate phase (dark gray phase *N* in Figs. 3a and 3c). Cesium is localized in the compound in separate inclusions (light spots in Fig. 3b) containing also phosphorus and oxygen. Wagh et al. [37] assumed previously that solidification of a cesium-containing solution in an MPP host material leads to the formation of the compound $Mg(Cs_xK_{1-x})·PO_4·6H_2O$. We have shown that the MPP-Cs sample after solidification of a concentrated cesium nitrate solution contains, along with cesium nitrate, also phosphate compounds (Fig. 1) that are formed by potassium replacement with cesium and are similar to K-struvite and newberite minerals, e.g., of the composition $Mg_{0.97}K_{0.29}Cs_{0.75}PO_4·6.3H_2O$ and $Mg_{0.55}K_{0.38}Cs_{0.77}·H_{0.75}PO_4·2.8H_2O$, respectively (Table 3). In addition, in the MPP-Cs sample there are areas containing up to

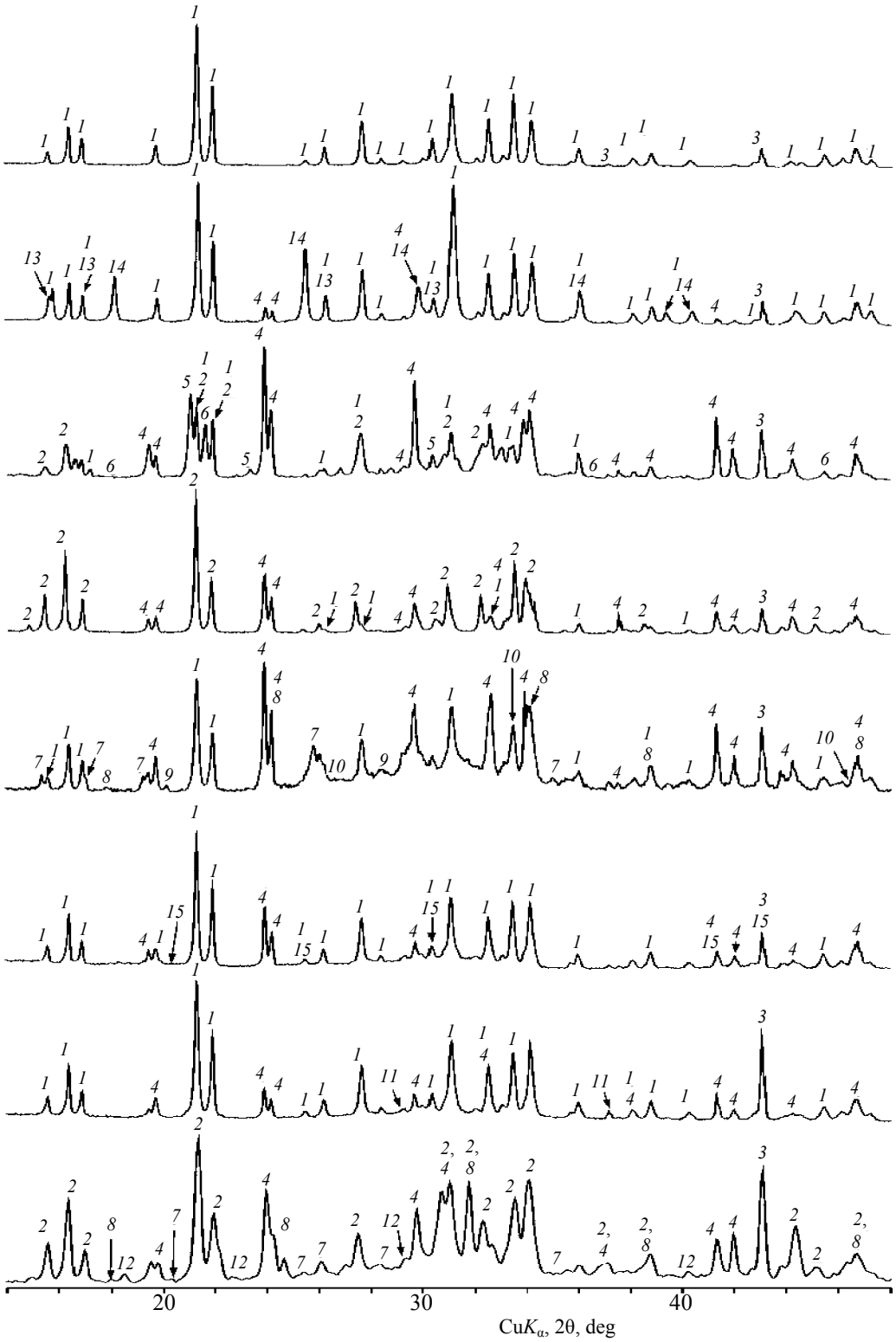

Fig. 1. X-ray diffraction patterns of the MPP host material and MPP compounds obtained by solidification of nitric acid solutions and simulated ILW solution (for solution compositions, see Table 1). Sample: (*I*) MPP host material, (*II*) MPP-Cs, (*III*) MPP-Na, (*IV*) MPP-NH_4, (*V*) MPP-Sr, (*VI*) MPP-La, (*VII*) MPP-Fe, and (*VIII*) MPP-ILW. Phase designations: (*1*) $MgKPO_4 \cdot 6H_2O$ (K-struvite), (*2*) $MgNH_4PO_4 \cdot 6H_2O$ (struvite), (*3*) MgO (periclase), (*4*) KNO_3 (niter), (*5*) $MgNaPO_4$, (*6*) Na_3PO_4 (olympite), (*7*) $MgHPO_4 \cdot 3H_2O$ (newberite), (*8*) KH_2PO_4, (*9*) $Sr(NO_3)_2$, (*10*) $Sr_3(PO_4)_2$, (*11*) $Fe_3(PO_4)O_3$ (grattarolaite), (*12*) NH_4NO_3 (nitramite), (*13*) $MgCsPO_4 \cdot 6H_2O$, (*14*) $CsNO_3$, and (*15*) $LaPO_4 \cdot 0.5H_2O$ (rhabdophane-La).

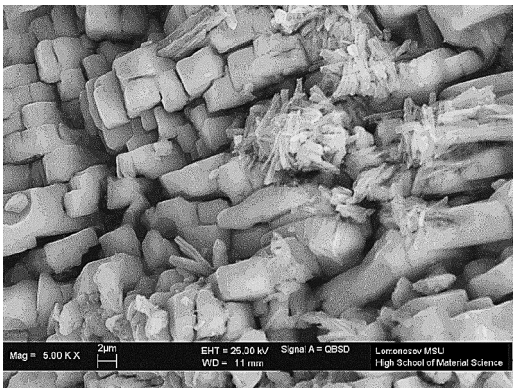

Fig. 2. SEM image of the MPP host material in backscattered electrons.

23.8 at. % cesium on the average (Table 3), which suggests the presence of fine Cs_3PO_4 particles in the compound.

The Sr distribution in the MPP-Sr sample (Fig. 3d) corresponds to the distribution of P and Mg, which confirms the formation of their phosphate compounds. Strontium is incorporated in K-struvite containing up to 5.5 at. % Sr (composition $Mg_{0.6}K_{0.23}Sr_{0.69}PO_{3.91}\cdot 6.1H_2O$, Table 3) and is also present in the form of $Sr_3(PO_4)_2$, which agrees with the data in Fig. 1. Lanthanum in MPP compound, similarly to Cs and Sr, is incorporated in a number of phosphates (MPP-La sample in Table 3), including analogs of K-struvite ($Mg_{0.60}K_{0.68}La_{0.36}PO_4\cdot 6.3H_2O$) and anhydrous mixed orthophosphate ($Mg_{0.55}K_{0.70}La_{0.44}PO_{4.06}$).

Thus, as demonstrated by the example of Cs, Sr, and La, RW radionuclides are immobilized in the MPP compound by chemical binding in the form of poorly soluble phosphates, which should ensure high resistance of the compound to leaching of these metals.

Mechanical Strength and Radiation and Heat Resistance of MPP Compounds

The compression strength of the prepared MPP compounds was 15 ± 3 MPa on the average. After 30 thermal cycles in the range from –40 to +40°C, 90-day immersion in water, or electron beam irradiation (dose 1 MGy), their strength decreased to 10 ± 2 MPa, which, nevertheless, meets the requirements [3] to the cement compound, no less than 5 MPa.

Introduction of 20–40 wt % mineral modifiers (wollastonite, bentonite, zeolite) into the compound enhances its mechanical strength (by a factor of 2–3)

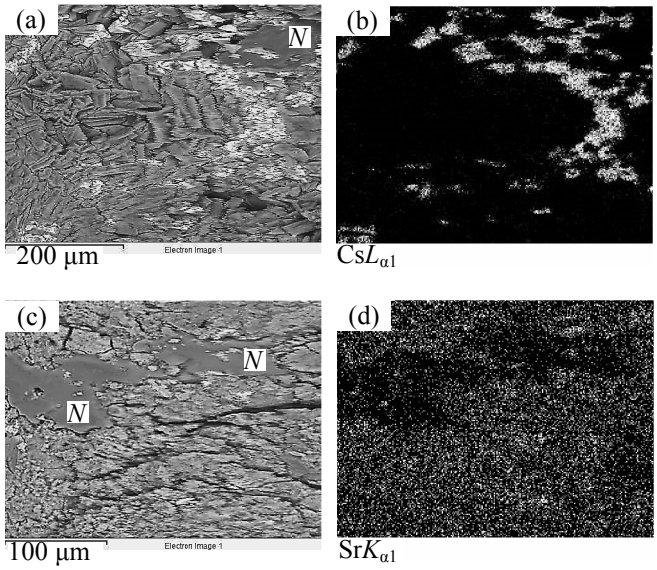

Fig. 3. SEM images of the (a) MPP-Cs and (b) MPP-Sr samples in backscattered electrons and elemental maps of (b) Cs and (d) Sr.

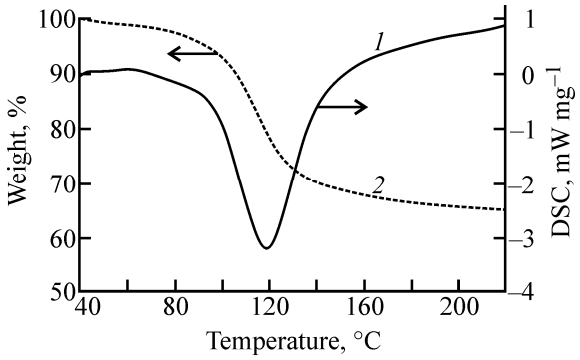

Fig. 4. Thermal behavior of the MPP host material. (*1*) DSC and (*2*) TG.

and heat resistance. For example, the compound containing 38 wt % wollastonite exhibited a strength of approximately 10 MPa even after heating for 4 h at 450°C. On the other hand, it is noted that the thermal action on the MPP compound is accompanied by the weight loss (Fig. 4, curve *2*), apparently, owing to dehydration. The endothermic effect corresponding to this process has a maximum at ~120°C (Fig. 4, curve *1*). Water was quantitatively removed from the samples in 24 h at 120°C and in 6 h at 180°C.

Thus, the use of dehydrated MPP compound for RW disposal will not lead to generation of dangerously explosive radiolytic hydrogen. It should also be noted that, according to our previous data [25], the radiochemical yield of hydrogen from the MPP compound

Table 4. Differential (numerator) and integral (denominator) leach rates of structure-forming elements from MPP compounds on the 28th day of contact with water, g cm^{-2} day^{-1}

Element	MPP	MPP-La	MPP-ILW
Mg	$7.7 \times 10^{-5}/2.3 \times 10^{-4}$	$3.4 \times 10^{-5}/2.3 \times 10^{-4}$	$1.3 \times 10^{-4}/8.2 \times 10^{-4}$
K	$1.2 \times 10^{-3}/5.8 \times 10^{-3}$	$1.4 \times 10^{-3}/9.3 \times 10^{-3}$	$9.6 \times 10^{-4}/1.2 \times 10^{-2}$
P	$5.5 \times 10^{-4}/3.2 \times 10^{-3}$	$8.7 \times 10^{-4}/2.0 \times 10^{-3}$	$5.1 \times 10^{-4}/3.9 \times 10^{-3}$
La	–	$6.4 \times 10^{-6}/1.3 \times 10^{-4}$	–

after solidification of simulated highly saline HLW is extremely low, 0.004 H_2 molecule per 100 eV. Similar effect was noted in [38] upon γ-irradiation of cement compounds incorporating simulated nitrate-containing RW, which was attributed to capture of radical products of water radiolysis by nitrate ions.

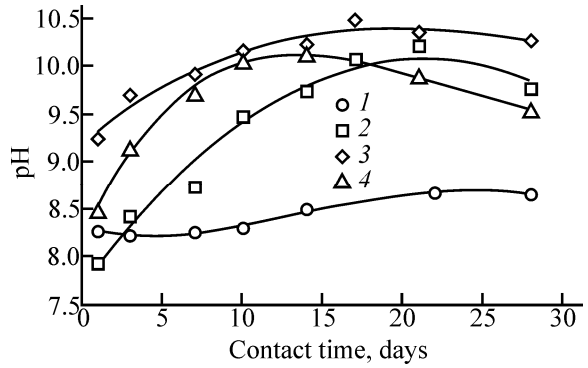

Fig. 5. pH of solutions after leaching MPP compounds as a function of the contact time with water. (*1*) MPP, (*2*) MPP-ILW, (*3*) MPP_wol, and (*4*) MPP-ILW_wol.

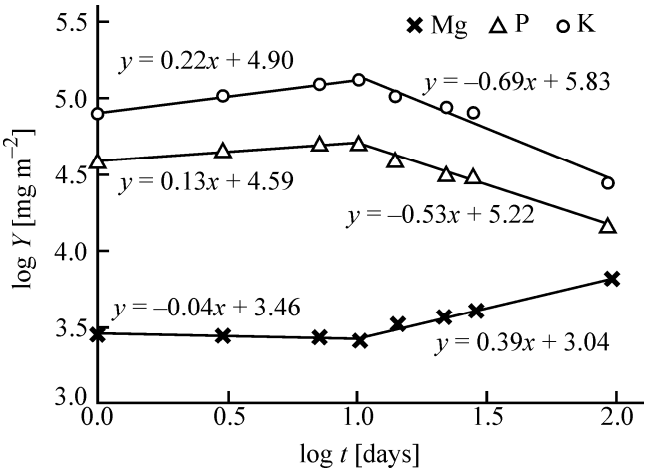

Fig. 6. The log–log plot of the yield *Y* of structure-forming elements of the MPP host material vs. contact time with water. The linear regression equations are given in the figure.

Hydrolytic Durability of MPP Compounds

The pH of the solutions after the contact of the MPP host material with double-distilled water, determined according to GOST (State Standard) R 52 126–2003, was 8.3–8.5 (curve *1* in Fig. 5). On the other hand, pH of the solutions after leaching MPP-ILW compound (curve *2* in Fig. 5) and compound samples with 38 wt % wollastonite (curves *3* and *4* in Fig. 5) increased to 9.5–10.5, which can be attributed to the hydrolysis of the formed readily soluble phosphate phases (e.g., Na_3PO_4) and wollastonite.

As we found, leaching of structure-forming elements of the MPP host material in the course of 90-day contact with water (Fig. 6) is controlled by different mechanisms. In the first 10 days, Mg, K, and P are washed out from the sample surface, with the coefficients *A* in Eqs. (2) equal to –0.04, 0.22, and 0.13, respectively. Stronger leaching of K and P compared to Mg can be attributed to the dissolution of residual unchanged KH_2PO_4. In the subsequent 80 days, the surface layer of the sample underwent gradual depletion of K and P (coefficients *A* –0.69 and –0.53, respectively), and the Mg leaching occurred via diffusion from the internal layers (*A* = 0.39).

Comparison of the hydrolytic durability data for different compounds (Table 4) shows that the influence of the chemical composition of the solidified solution on leaching of the structure-forming elements of the MPP host material is insignificant. The differential leach rate of Mg, K, and P does not exceed 1.3×10^{-4}, 1.4×10^{-3}, and 8.7×10^{-4} g cm^{-2} day^{-1}, respectively. An increase in the integral leach rate of K from MPP-ILW and MPP-La and of Mg from MPP-ILW, compared to straight MPP (Table 4), can be attributed to possible formation and leaching or dissolution in the first day of contact of the samples with water of separate compounds of these elements, primarily KNO_3, and also, possibly, $Mg(H_2PO_4)_2 \cdot xH_2O$, $Mg_3(PO_4)_2 \cdot xH_2O$, and $Mg_2PO_4(OH)$.

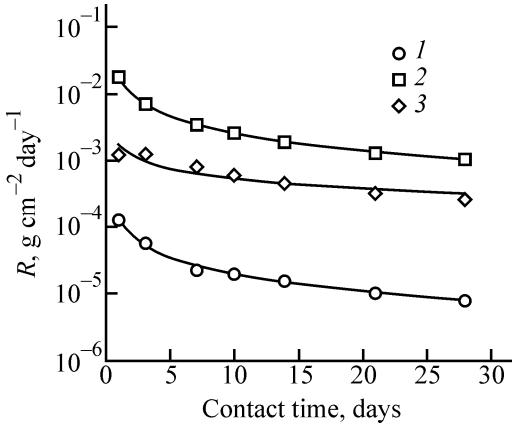

Fig. 7. Integral leach rate R of (*1*) ^{239}Pu and (*2*) ^{152}Eu from MPP-ILW samples and of ^{152}Eu from the sample containing 38 wt % wollastonite (MPP-ILW_wol).

The MPP compound exhibits high hydrolytic durability with respect to the radionuclide leaching (Fig. 7), which is the main criterion of its suitability for RW storage/disposal. The differential and integral leach rates from an MPP-ILW sample on the 28th day of contact with water were 2.1×10^{-6} and 8.1×10^{-6} for ^{239}Pu, and 1.4×10^{-4} and 1.1×10^{-3} g cm^{-2} day^{-1} for ^{152}Eu, respectively. On the other hand, introduction of wollastonite into the compound (Fig. 7, curve *3*) leads to a decrease in the differential and integral ^{152}Eu leach rates to 6.5×10^{-5} and 2.6×10^{-4} g cm^{-2} day^{-1}, respectively.

Thus, our studies show that high physicochemical stability and hydrolytic durability of MPP compound make it promising for industrial solidification of RW, including actinide-containing ILW of complex chemical composition.

ACKNOWLEDGMENTS

Determination of element concentrations in solutions by ICP-AES was performed at the Laboratory of Methods for Investigation and Analysis of Substances and Materials, Vernadsky Institute of Geochemistry and Analytical Chemistry, Russian Academy of Sciences (I.N. Gromyak, E.M. Sedykh). Experiments were performed with an Ultima-IV X-ray diffractometer (Rigaku) purchased within the framework of implementation of the Development Program of the Moscow State University.

The study was financially supported by the Russian Science Foundation (project no. 16-13-10539).

REFERENCES

1. *Radioactive Waste Forms for the Future*, Lutze, W. and Ewing, R.C., Eds., Amsterdam: Elsevier, 1988.
2. Stefanovsky, S.V., Yudintsev, S.V., Vinokurov, S.E., and Myasoedov, B.F., *Geochem. Int*., 2016, vol. 54, no. 13, pp. 1136–1156.
3. *NP-019-15*: Federal regulations and rules in the field of using atomic energy. Collection, processing, storage, and conditioning of liquid radioactive waste. Safety requirements.
4. Kozlov, P.V. and Gorbunova, O.A., *Tsementirovanie kak metod immobilizatsii radioaktivnykh otkhodov* (Cementation as a Method for Radioactive Waste Immobilization), Ozersk: Mayak, 2011.
5. Sobolev, I.A., Ozhovan, M.I., Shcherbatova, T.D., and Batyukhnova, O.G., *Stekla dlya radioaktivnykh otkhodov* (Glasses for Radioactive Waste), Moscow: Energoatomizdat, 1999.
6. Stefanovsky, S.V., Stefanovskaya, O.I., Vinokurov, S.E., et al., *Radiochemistry*, 2015, vol. 57, no. 4, pp. 348–355.
7. Glagolenko, Yu.V., Drozhko, E.G., and Rovnyi, S.I., *Vopr. Radiats. Bezopasn.*, 2006, no. 1, pp. 23–34.
8. Ringwood, A.E., Kesson, S.E., Reeve, K.D., et al., *Radioactive Waste Forms for the Future*, Lutze, W. and Ewing, R.C., Eds., Amsterdam: Elsevier, 1988, pp. 233–334.
9. Laverov, N.P., Sobolev, I.A., Stefanovsky, S.V., et al., *Dokl. Ross. Akad. Nauk*, 1998, vol. 362, pp. 670–672.
10. Vinokurov, S.E., Kulyako, Yu.M., Perevalov, S.A., and Myasoedov, B.F., *C. R. Chim*., 2007, vol. 10, nos. 10–11, pp. 1128–1130.
11. Petrov, Yu.B., *Induktsionnaya plavka okislov* (Induction Melting of Oxides), Moscow: Nauka, 1983.
12. Merzhanov, A.G., *Russ. Chem. Rev.*, 2003, vol. 72, no. 4, pp. 289–310.
13. Kurkumeli, A.A., Molokhov, M.N., Sadkovskaya, O.D., et al., *At. Energ.*, 1992, vol. 73, pp. 210–215.
14. Wagh, A.S., *Chemically Bonded Phosphate Ceramics. Twenty-First Century Materials with Diverse Applications*, Elsevier, 2004.
15. Roy, D.M., *Science*, 1987, vol. 235, no. 4789, pp. 651–658.
16. Aloy, A.S., Kovarskaya, E.N., Kol'tsova, T.I., et al., RF Patent 2 137 229, Priority of Nov. 20, 1997.
17. Choi, J., Um, W., and Choung, S., *J. Nucl. Mater*., 2014, vol. 452, pp. 16–23.
18. Filippov, Ya.Yu., Larionov, D.S., Putlyaev, V.I., et al., *Glass Ceram*., 2013, vol. 70, nos. 7–8, pp. 306–310.
19. Graeser, S., Postl, W., Bojar, H.-P., et al., *Eur. J. Mineral*., 2008, vol. 20, no. 4, pp. 629–633.
20. Sharygin, L.M., *Fosfatnye tsementy v atomnoi ener-*

getike (Phosphate Cements in Atomic Power Engineering), Yekaterinburg: Ural'skoe Otdel. Ross. Akad. Nauk, 2015.

21. Wagh, A.S., Sayenko, S.Yu., Dovbnya, A.N., et al., *J. Nucl. Mater*., 2015, vol. 462, pp. 165–172.
22. Borzunov, A.I., D'yakov, S.V., and Poluektov, P.P., *At. Energy*, 2004, vol. 96, no. 2, pp. 123–126.
23. Sukhonosov, V.Ya., Nikolaev, A.N., Nikolaev, S.A., et al., *Ross. Khim. Zh.*, 2010, vol. LIV, no. 3, pp. 89–93.
24. Myasoedov, B.F., Kalmykov, S.N., Kulyako, Yu.M., and Vinokurov, S.E., *Geochem. Int*., 2016, vol. 54, no. 13, pp. 1157–1168.
25. Vinokurov, S.E., Kulyako, Yu.M., Slyunchev, O.M., et al., *Radiochemistry*, 2009, vol. 51, no. 1, pp. 65–72.
26. Vinokurov, S.E., Kulyako, Yu.M., and Myasoedov, B.F., *Ross. Khim. Zh.*, 2010, vol. LIV, no. 3, pp. 81–88.
27. Vinokurov, S.E., Kulyako, Yu.M., Slyuntchev, O.M., et al., *J. Nucl. Mater.*, 2009, vol. 385, pp. 189–192.
28. Vinokurov, S.E., Kulyako, Yu.M., and Myasoedov, B.F., RF Patent 2 381 580, Priority of Oct. 13, 2008.
29. *FR.1.28.2014.18 803, MI-171-13:* Procedure for measuring the ultimate strength of cement compounds incorporating radioactive waste using a Testing Sybertronic testing machine.
30. *MPI-04-12:* Determination of the frost resistance of cement compounds incorporating RW in an MK-53 climatic chamber.
31. *GOST* (State Standard) *R 52126–2003:* Radioactive waste. Determination of the chemical durability of solidified high-level waste by prolonged leaching, Moscow: Gosstandart Rossii, 2003.
32. De Groot, G.J. and van der Sloot, H.A., *Stabilization and Solidification of Hazardous, Radioactive, and Mixed Wastes: ASTMSTP 1123*, Gilliam, T.M. and Wiles, G., Eds., Philadelphia: ASTM, 1992. vol. 2, pp. 149–170.
33. Al-Abed, S.R., Hageman, P.L., Jegadeesan, G., et al., *Sci. Total Environ*., 2006, vol. 364, pp. 14–23.
34. Moon, D.H. and Dermatas, D., *Eng. Geol*., 2006, vol. 85, pp. 67–74.
35. Torras, J., Buj, I., Rovira, M., and de Pablo, J., *J. Hazard. Mater*., 2011, vol. 186, pp. 1954–1960.
36. Xue, Q., Wang, P., Li, J.-S., et al., *Chemosphere*, 2017, vol. 166, pp. 1–7.
37. Wagh, A.S., Sayenko, S.Y., Shkuropatenko, V.A., et al., *J. Hazard. Mater*., 2016, vol. 302, pp. 241–249.
38. Ershov, B.G., Yurik, T.K., Bykov, G.L., et al., *Vopr. Radiats. Bezopasn.*, 2008, no. 1, pp. 3–15.

Translated by G. Sidorenko